

Thermochemistry of nanoparticles on a substrate: Zinc oxide on amorphous silica

Tatiana Y. Shvareva, Sergey V. Ushakov, and Alexandra Navrotsky^{a)}
*Peter A. Rock Thermochemistry Laboratory, University of California at Davis,
Davis, California 95616*

Joseph A. Libera and Jeffrey W. Elam
Argonne National Laboratory, Argonne, Illinois 60439

(Received 3 February 2008; accepted 21 March 2008)

Crystalline samples of zinc oxide on a mesoporous amorphous silica substrate were prepared by 5 to 15 atomic layer deposition cycles with diethyl zinc and water at 150 °C. Samples were characterized by x-ray diffraction, thermogravimetry, and nitrogen adsorption–desorption isotherms. High-temperature oxide melt solution calorimetry and water adsorption calorimetry experiments were performed to measure surface enthalpy for crystalline ZnO particles supported on the substrate. The measured enthalpies 1.23 ± 0.35 and 2.07 ± 0.59 J/m² for hydrous and anhydrous surfaces, respectively, are in agreement with previously reported measurements for unsupported ZnO nanoparticles. Feasibility of thermochemical characterization of complex system of atomic layer deposition (ALD) prepared particles on a substrate was demonstrated.

I. INTRODUCTION

The nonnegligible contribution of surface and interfacial terms is a characteristic feature of any thermodynamic description of nanomaterials. High-temperature oxide melt solution calorimetry has proved to be one of the most versatile methods to measure surface enthalpies of unsupported metal oxide nanoparticles.^{1–10} One of the most significant findings of such calorimetric experiments is strong evidence that changes in the bulk crystal structure of nanophases (polymorphism) observed for alumina,² zirconia,³ and titania⁴ are caused by the lower surface enthalpies of the metastable phase overriding its bulk instability. In thermodynamic analyses of nanostructures, three main factors must be addressed: (i) effect of synthesis method and surface morphology on surface energies, (ii) contribution from interfacial energies, and (iii) effect of adsorption of H₂O or other molecules on the surface or interface.

Nanoparticles in both natural and synthetic settings often form complex structures: core shell particles, adsorbed layers of molecules or particles on the surface of parent nanoparticles, and corrosion layers. Their structures contain several kinds of interfaces: particle–air, particle–water, and particle–particle. To understand these complex interactions, it is instructive to study a model

system, intermediate in complexity between isolated nanoparticles and real-world multicomponent and multiphase nanophase systems.

We report a study of zinc oxide deposited by atomic layer deposition (ALD)¹¹ on a commercial amorphous silica substrate (Silicycle). There is widespread use of amorphous SiO₂ as a substrate for catalysis^{12–14} and application of ZnO to catalyze methanol synthesis.^{15–17} This system is appropriate for calorimetric study for several reasons. First, there are no polymorphic transformations or oxidation state changes during heating ZnO up to its melting temperature. Second, surface energies of dry and hydrous crystalline zinc oxide and amorphous silica were measured previously.^{9,18} Finally, to the best of our knowledge, it is the first report of calorimetric study for any nanoparticle/substrate system that resembles the actual complexity of nanoscale systems in technology.

II. EXPERIMENTAL METHODS

Amorphous silica used as a substrate for deposition (Silicycle 10040M)¹³ was commercially obtained from Silicycle Company (Quebec City, Canada). Brunauer–Emmett–Teller (BET) surface area 94.9 ± 0.6 m²/g and Barret–Joyner–Halenda (BJH) average pore size 26 ± 3 nm, obtained from the nitrogen adsorption isotherm, agreed with the specifications provided with the material. The substrate Silicycle (SIL) consisted of particles of mesoporous material 50 to 100 μm in diameter. Atomic layer deposition of ZnO, electron microscopy, and x-ray

^{a)}Address all correspondence to this author.
e-mail: anavrotsky@ucdavis.edu
DOI: 10.1557/JMR.2008.0237

fluorescence analysis were performed at Argonne National Laboratory. X-ray diffraction (XRD), thermogravimetry (TG), nitrogen and water adsorption, and calorimetry were performed at University of California at Davis.

A. Atomic layer deposition

The viscous flow reactor used for deposition is described in detail elsewhere.^{19–21} Zinc oxide was deposited by multiple alternating exposure of substrate to gaseous diethyl zinc and water. Deposition was performed at 150 °C to prevent the formation of zinc metal particles from the decomposition of diethyl zinc above 175 °C.¹¹ Five deposition cycles produced an amorphous zinc oxide, which was crystallized to wurtzite structure upon annealing at 450 °C for 2 h in oxygen, as proved by XRD measurements. Ten and fifteen deposition cycles produced crystalline ZnO (wurtzite). All crystalline samples will be called ZnO(*n*) with *n* being the number of deposition cycles. Part of ZnO(10) and ZnO(15) samples were annealed under similar conditions to ensure 100% crystalline ZnO and full oxidation of Zn metal. Transmission electron microscopy (TEM) performed on similar samples¹¹ revealed that in the early stages of growth, zinc oxide ALD on Silicycle does not produce uniform film coatings, but results in the formation of nanoparticles.

B. X-ray fluorescence (XRF)

The amount of deposited ZnO was measured by XRF analysis with an ED2000 system (Oxford Instruments, Buckinghamshire, UK) using standards prepared by mixing known amounts of ZnO (NanoTek ZnO, 24–71 nm, Nanophase Technologies Corp., Burr Ridge, IL) with Silicycle. Obtained values were corrected for water content in Silicycle and recalculated to the molar ZnO:SiO₂ ratio.

C. XRD

XRD analysis was performed on all as-received and annealed samples with a Scintag PAD V diffractometer (Cupertino, CA) at 45 kV and 40 mA using Cu K_α ($\lambda = 1.54056 \text{ \AA}$) radiation at two theta angles between 10° and 90°. Lattice parameters and crystallite size for ZnO were identified by a full-profile (Rietveld) refinement routine as implemented in JADE 6.1 (Materials Data Inc., Livermore, CA) software.

D. Thermogravimetry

Water content in pure Silicycle and in all the samples was determined by thermogravimetric analysis (TGA) with a Netzsch (Selb, Germany) STA 449 system under oxygen flow of 40 mL/min and a heating rate of 10 K/min.

Prior to analysis, samples were equilibrated at 50% relative humidity at 25 °C in lab air.

E. Oxide melt solution calorimetry

Enthalpies of drop solution of crystalline ZnO(*n*) samples, bare amorphous silica substrate, and bulk ZnO with wurtzite structure, were measured in a custom-built Tian–Calvet twin microcalorimeter at 702 °C using lead borate (2PbO–B₂O₃) as a solvent. Air was flushed through the calorimeter glassware assembly at 35 mL/min to expel water vapor evolved upon sample dissolution. Air was also bubbled through the melt at 4 mL/min to prevent local saturation and facilitate dissolution of the sample. The samples were pressed into pellets of mass ~10 mg, weighed on a microbalance and dropped from room temperature into the solvent. The calorimeter was calibrated using the heat content of 15 mg pellets of corundum. The overall methodology of calibrations and measurements has been described previously^{22,23} and is well established.

F. Nitrogen adsorption isotherms and water adsorption calorimetry

Total surface area of the samples and pore-size distributions were evaluated from the full adsorption–desorption isotherms of N₂ at 196 K collected for all samples using a Micromeritics (Norcross, GA) ASAP2020 instrument. Surface area of the samples was calculated from the BET equation using five points of adsorption data in the 0.05 to 0.35 *P*/*P*₀ region relative pressure.²⁴ Pore size was calculated with BJH model from desorption data.²⁵

Prior to isotherm collection and water adsorption calorimetry, all samples were degassed at the annealing temperature of 450 °C for 4 h under vacuum and cooled under an oxygen atmosphere to produce crystalline ZnO. Part of amorphous as-prepared ZnO(5)am sample was degassed only at its deposition temperature (150 °C) under the same conditions.

Enthalpy of water adsorption was measured with a commercial Calvet type microcalorimeter (Setaram DSC111, Caluire, France) coupled with a Micromeritics ASAP 2020 gas adsorption system. The instrumentation and technique are described in detail elsewhere.²⁶ After evacuation, doses of about 5 mmol of H₂O vapor were introduced into the fork-type sample holder, according to a prescribed program, and the absorbed amounts were determined from the pressure drop. Heat of adsorption for each dose was derived by integration of the calorimetric peak, applying a calibration factor from the fusion enthalpy of gallium. A correction for water adsorption on the sample holder and manifold was applied to integral values from a run with an empty sample tube. To estimate experimental uncertainties, two to three runs of

water adsorption were performed on each sample, with degas after each run.

III. RESULTS

A. XRD

Results of analysis of crystallite size from XRD patterns are presented in Table I together with composition and measured total BET surface areas of the samples. Powder x-ray diffraction analysis of as-received samples did not reveal metallic Zn in any samples; crystalline ZnO (wurtzite) was detected in the samples with 10 and 15 deposition cycles [ZnO(10) and ZnO(15)] (Fig. 1). Average size of diffracting domains in these as-prepared samples was refined as ~ 3 and ~ 4 nm, respectively. No crystalline phase was detected in as-prepared sample with five deposition cycles ZnO(5)am (Fig. 1).

B. Nitrogen adsorption

Nitrogen adsorption–desorption isotherms for all samples are represented in Fig. 2. All isotherms belong to type IV in the IUPAC classification related to capillary condensation within the mesopores.²⁷ All isotherms have a hysteresis loop that can be identified as type H2. This type of hysteresis is usually associated with gas adsorption within a network of pores with geometry that can be described as pores with narrower neck and wider body.²⁷ The inset in Fig. 2 shows the distribution of pore size for each sample. BJH analysis of the isotherms yields the pore diameter of bare substrate as 26 ± 3 nm (Table I), consistent with 30 nm value claimed by the manufacturer. After ZnO deposition, average pore size decreases to 19 nm for amorphous as-deposited ZnO(5)am sample and to 14.5 to 15.6 nm for all crystalline samples after degas at 450 °C.

C. Water adsorption calorimetry

Enthalpies of water adsorption versus adsorbed amounts are shown in Fig. 3. Based on TG, all residual water left after degas at 450 °C is attributed to Silicycle, as shown in the thermodynamic cycle (Table II), and initial surface coverage of ZnO is taken as zero. We consider the residual water amount from TG experiments as a constant amount of water that is left on the pure

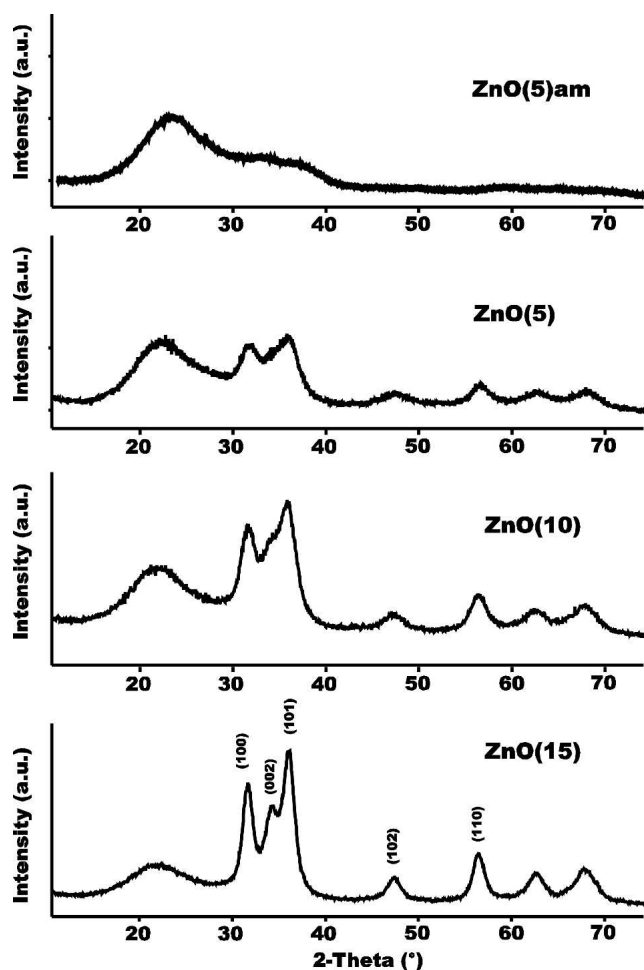


FIG. 1. Powder XRD patterns ($\text{Cu K}\alpha$ radiation). ZnO(5)am: as-received amorphous ZnO after five deposition cycles. ZnO(5), ZnO(10), ZnO(15): crystalline ZnO after annealing at 450 °C in O_2 .

substrate after prolonged exposure to the temperature of deposition, 150 °C. Any excess over this amount, linearly increasing with ZnO surface area, is attributed to the hydration of the ZnO surface.

This water distribution is consistent with a thermogravimetric experiment on unsupported ZnO nanoparticles (Nanophase Technologies Corp.), which lost 0.6 wt% of total weight after holding at 450 °C for 4 h and only 0.06 wt% after heating from 450 to 900 °C. Part of the weight loss on heating to 900 °C might be attributed

TABLE I. Sample composition, crystallite size, water content, surface area, and pore size from nitrogen adsorption.

ID ^a	ZnO (wt%)	mH ₂ O ^b	xSiO ₂ ^b	Anneal <i>T</i> (°C)	ZnO crystallite size (Å) ^c	BET SA (m ² /g)	BJH pore diameter (Å)
ZnO(5)am	21.6	0.72	3.89	150	...	75.6 ± 1.5	190 ± 4
ZnO(5)	21.6	0.54	3.94	450	.../34(3)	79.9 ± 0.4	156 ± 4
ZnO(10)	41.4	0.33	1.80	450	30(5)/36(5)	66.3 ± 0.5	147
ZnO(15)	51.6	0.20	1.20	450	40(2)/55(7)	51.2 ± 0.6	145 ± 9
Silicycle	0	96.8 ± 0.8	262 ± 29

^aNumber of deposition cycles is given in the parenthesis, all samples except ZnO(5)am were annealed at 450 °C.

^bSee Table IV.

^cAs prepared/after anneal.

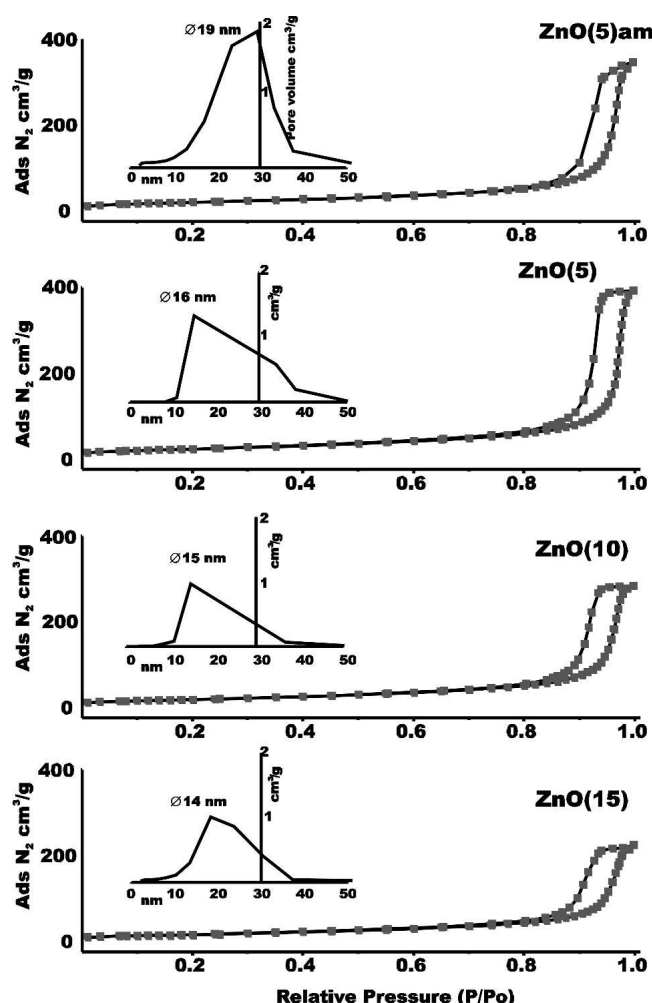


FIG. 2. Full N_2 adsorption-desorption isotherms collected at 77 K. Insets show the pore-size distribution and average pore size calculated from BJH model from the desorption branch. ZnO(5)am: as-received amorphous ZnO after five deposition cycles. ZnO(5), ZnO(10), ZnO(15): crystalline ZnO after degas at 450 °C and exposure to O_2 .

to sublimation of ZnO itself, since weight loss does not stabilize at this temperature.

ZnO(5)am was degassed at 150 °C, and it retained more water than can be attributed to Silicycle. This water corresponds to initial coverage of 4 $\text{H}_2\text{O}/\text{nm}^2$ on the ZnO surface. The area under the curve in Fig. 3 corresponds to the integral adsorption enthalpy at given coverage (Table III). These values are used in the thermochemical cycle (ΔH_4 in Table I) to obtain excess enthalpy of anhydrous crystalline ZnO coatings relative to bulk material.

D. Oxide melt solution calorimetry

Drop-solution enthalpies of crystalline samples, uncoated Silicycle, and bulk zinc oxide were measured to calculate interfacial enthalpies of ZnO coatings (Table III). Samples were equilibrated at 50% RH at 25 °C before calorimetry and thermogravimetric experiments.

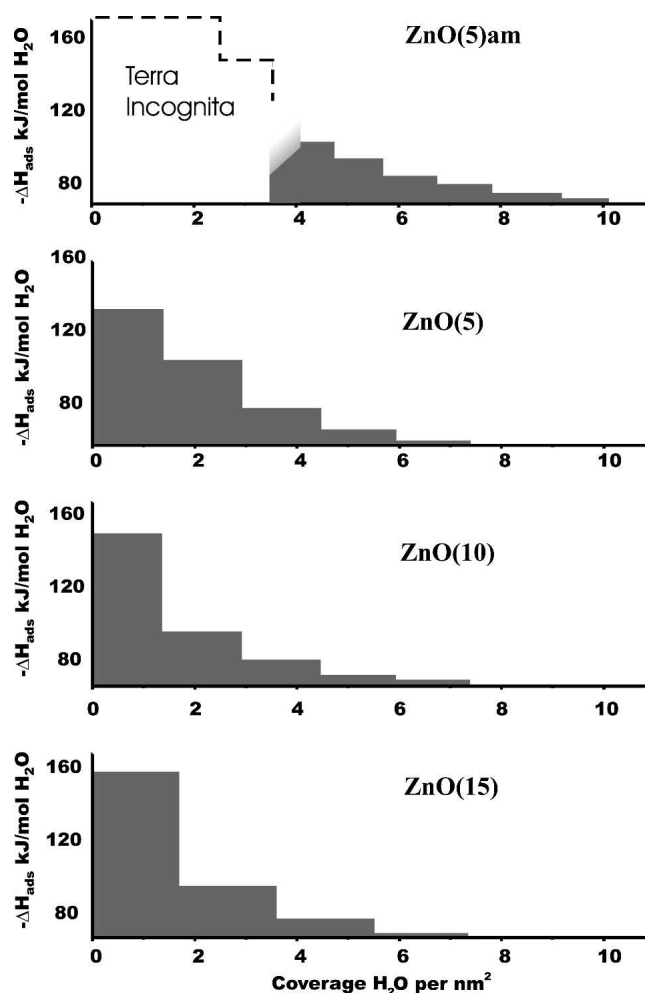


FIG. 3. Enthalpy of water adsorption as a function of water coverage of the surface. ZnO(5)am: as-received amorphous ZnO after five deposition cycles. ZnO(5), ZnO(10), ZnO(15): crystalline ZnO after degas at 450 °C and exposure to O_2 . Intercept with y axis corresponds to the enthalpy of water condensation at room temperature (-44 kJ/mol). Each step represents an enthalpy of adsorption of each dose of water vapor. The area is proportional to ΔH_4 in Table IV. Surface area used in the calculations of coverage of ZnO(5)am corresponds to measured BET surface area. For ZnO(5), SA_{ZnO} calculated by Eq. (2). For ZnO(10) and ZnO(15) surface area SA_{ZnO} normalized from water coverage of ZnO(5).

The data for bulk ZnO and amorphous silica are in good agreement with previously reported values.^{28,29} The enthalpy of drop solution of each sample includes components related to ZnO coatings, Silicycle substrate, and adsorbed water. The constant water content in the substrate was determined by TGA to be 0.04 mol of H_2O per mol of Silicycle.

For the calculations of hydrated surface enthalpies, all adsorbed water is corrected for as energetically equivalent to liquid water. For the anhydrous surface, measured integral adsorption enthalpies $\Delta H_{\text{ads}} = \Delta H_4$, are accounted for in the thermochemical cycle. ΔH_5 and ΔH_6 are reference values.³⁰

TABLE II. Thermochemical cycle for the calculation of excess enthalpy of ZnO coatings.

1. $\text{ZnO} \cdot m\text{H}_2\text{O}_{\text{ads(SA,298)}} +$ $x(\text{SiO}_2 \cdot 0.04\text{H}_2\text{O})_{\text{(s,298)}} \rightarrow \text{solution}$ $+ (0.04x + m) \cdot \text{H}_2\text{O}_{\text{(g,975)}}^{\uparrow}$	$\Delta H_1 = \Delta H_{\text{ds sample}}$
2. $\text{SiO}_2 \cdot 0.04\text{H}_2\text{O}_{\text{(SA,298)}} \rightarrow$ $\text{solution} + 0.04\text{H}_2\text{O}_{\text{(g,975)}}^{\uparrow}$	$\Delta H_2 = \Delta H_{\text{ds Silicycle}}$
3. $\text{ZnO}_{\text{(bulk,298)}} \rightarrow \text{solution}$	$\Delta H_3 = \Delta H_{\text{ds ZnO (bulk)}}$
4. $\text{ZnO}_{\text{(SA,298)}} + m \cdot \text{H}_2\text{O}_{\text{(g,298)}} \rightarrow$ $\text{ZnO} \cdot m\text{H}_2\text{O}_{\text{ads(SA,298)}}$	$\Delta H_4 = \Delta H_{\text{ads}}$
5. $\text{H}_2\text{O}_{\text{(g,298)}} \rightarrow \text{H}_2\text{O}_{\text{(g,975)}}^{\uparrow}$	$\Delta H_5 = 25.01 \text{ kJ/mol}^a$
6. $\text{H}_2\text{O}_{\text{(l,298)}} \rightarrow \text{H}_2\text{O}_{\text{(g,298)}}^{\uparrow}$	$\Delta H_6 = 44.00 \text{ kJ/mol}^a$
7. $\text{ZnO}_{\text{(bulk,298K)}} \rightarrow \text{ZnO}_{\text{(SA,298)}}$	$\Delta H_7 = \text{excess w.r.t. bulk ZnO}$

$$\Delta H_7 = -\Delta H_1 + x\Delta H_2 + \Delta H_3 - \Delta H_4 + m \cdot \Delta H_5.$$

For hydroxylated surface $\Delta H_4 = -m \cdot \Delta H_6$.

For anhydrous surface, $\Delta H_4 = \Delta H_{\text{adsorption as measured}}$.

^aRef. 30.

In the thermochemical cycle, we correct for the substrate contribution by subtraction of heat of drop solution of hydrated Silicycle from the sample drop solution enthalpy on the wt% basis. By doing this, for fully coated Silicycle we effectively assume that ZnO–Silicycle interfacial enthalpy is close to the enthalpy of the Silicycle–air (SIL–air) interface. Silicycle is mesoporous amorphous hydrous silica, and energy for this interface is remarkably small and was calorimetrically measured previously (0.129 J/m^2).¹⁸ The ZnO–Silicycle interfacial energy is likely to be somewhat larger than this value. We performed calculations, assuming that it is five times larger, and the resulting excess enthalpies changed by less than the experimental uncertainty.

IV. DISCUSSION

A. Morphology of ZnO coatings

Application of different numbers of cycles of ZnO deposition on the surface of porous amorphous silica provided the series of samples with varying ZnO:SiO₂ molar ratio and different interface areas. Crystalline ZnO deposited by ALD does form particles on the substrate. This behavior is observed by TEM,¹¹ corroborated by our BJH pore size measurements after deposition, and expected from the extremely low SIL–air interface energy of hydroxylated SiO₂ of 0.129 J/m^2 .¹⁸

Our finding of amorphous ZnO in as-prepared ZnO(5)am sample is consistent with previous reports that below 9 ALD cycles amorphous ZnO can be obtained.^{20,21} After annealing at 450°C , $\sim 3 \text{ nm}$ crystallites (estimated from XRD peak broadening, Table I) were detected in the ZnO(5) sample, indicating crystallization. After annealing at 450°C , average crystallite size in ZnO(10) increased from 3 to $\sim 3.6 \text{ nm}$ and in and ZnO(15) is from 4 to 5.5 nm . Crystallite size in ZnO(15) sample ($5.5 \pm 0.7 \text{ nm}$) agrees well with the size of the ZnO particles $\sim 5 \text{ nm}$, measured by TEM for a similar sample.¹¹

B. Water adsorption calorimetry

The primary purpose of water adsorption calorimetry on crystalline samples in this work is to provide data for thermochemical cycles from which surface enthalpies for anhydrous surfaces could be derived. Experiments were also performed on as-prepared samples after five deposition cycles with amorphous ZnO [ZnO(5)am]. In Fig. 3 enthalpies of water adsorption per dose are plotted versus coverage. Since sample size and adsorbed amount per dose ($\sim 5 \text{ mmol H}_2\text{O}$) were kept constant, the coverage and adsorption enthalpy per dose varied depending on sample surface area and, in case of amorphous ZnO, adsorption mechanism. It is remarkable though, that integral adsorption enthalpy at coverage corresponding to liquid water level (-44 kJ/mol , the point at which the heat of adsorption reaches heat of water condensation) for all crystalline samples converges to $-80 \text{ kJ/mol H}_2\text{O}$ within calculated uncertainties. This observation suggests that differences between samples in the surface area of uncovered Silicycle do not affect adsorption enthalpies calculations substantially, since the same correction for volumes adsorbed in an experiment with an empty tube was applied for all samples. Thus, adsorbed amounts of water to reach the enthalpy of water condensation at room temperature (-44 kJ/mol) was used to estimate surface area of ZnO in samples ZnO(10) and ZnO(15) as described in the next section.

Integral adsorption enthalpy for amorphous ZnO, obtained after five deposition cycles, cannot be calculated from our experiment because of initially adsorbed water that cannot be desorbed completely without crystallizing the coating. The adsorption enthalpy reaches -44 kJ/mol at a surface coverage of $7.4 \text{ H}_2\text{O/nm}^2$ for the crystalline ZnO(5) sample and at $10.2 \text{ H}_2\text{O/nm}^2$ for the amorphous ZnO(5)am, when initially preadsorbed water is taken into account. The surface area of ZnO in the amorphous sample is taken equal to the BET surface area. If the actual surface area is smaller, the difference in coverage would be even more substantial. Water dissociation on crystalline ZnO is a possible explanation. It was suggested for iron oxides³¹ that water adsorption takes place through a different mechanism on the surface of crystalline and amorphous samples. Differences in coverage that we observe support this hypothesis.

C. Interface area calculations

Several types of interfaces exist in our samples: (i) ZnO–air interface on the exposed surface of zinc oxide (labeled further as SA_{ZnO}); (ii) hydrated SiO₂–air interface on the uncoated substrate (labeled further as SA_{SiO_2}); (iii) ZnO–Silicycle interface formed on the contact of ZnO nanocrystals with the substrate (labeled further as $\text{IA}_{\text{SiO}_2\text{-ZnO}}$); and (iv) ZnO–ZnO interface formed on the contact of nanocrystals.

TABLE III. Measured and calculated interface areas of the samples per mol of ZnO.

Sample	SA_{BET}	$IA_{\text{ZnO(XRD)}}$	$IA_{\text{ZnO(XRD)}}$ $\times 10^3 \text{ m}^2/\text{mol ZnO}$	SA_{ZnO}	SA_{SiO_2}
ZnO(5)	26.4 ± 0.2	25.6 ± 2.3	11.7 ± 1.1	13.9 ± 2.6	12.5 ± 1.1
ZnO(10)	13.0 ± 0.1	24.2 ± 3.4	11.1 ± 1.7	8.8^a	-0.95 ± 1.7
ZnO(15)	8.1 ± 0.1	15.8 ± 2.1	7.6 ± 1.0	5.5^a	-0.2 ± 1.0

^aCalculated from water adsorption data, see text for details.

TABLE IV. High-temperature drop-solution calorimetry and adsorption calorimetry data.

Samples	ΔH_{ds} , ($2\text{PbO} \cdot 3\text{B}_2\text{O}_3$ J/g of sample) ^a	Average coverage at liquid water level ($\text{H}_2\text{O}/\text{nm}^2$)	Integral heat of adsorption at coverage corresponding to liquid water level (kJ/mol H_2O) ^a	Excess enthalpy (ΔH_7 , kJ/mol ZnO hydrous surface)	Excess enthalpy (ΔH_7 kJ/mol ZnO anhydrous surface)
ZnO(5)	$609.4 \pm 10.2(8)$	7.4	$-80.2 \pm 2.5(3)$	17.5 ± 3.8	27.9 ± 3.8
ZnO(10)	$646.4 \pm 9.7(8)$	7.4^b	$-80.5 \pm 0.9(3)$	6.6 ± 2.8	10.8 ± 2.8
ZnO(15)	$640.3 \pm 7.9(8)$	7.4^b	$-87.2 \pm 8.5(3)$	3.8 ± 1.4	6.7 ± 1.5
ZnO(bulk)	$626.8 \pm 4.4(8)$
Silicycle	$540.8 \pm 6.5(8)$

^aUncertainties are calculated as two standard deviations of the mean. Number of experiments is given in parentheses.^bCoverage taken equal to those of ZnO(5) to calculate surface area of ZnO from water adsorption, see text for details.

We cannot measure directly the areas of each interface. However, from BET measurements we know surface area of Silicycle substrate before coating (SA_{SIL}) and from XRF analysis we determined Silicycle weight fraction in each sample. We also know BET surface area of the samples after ZnO deposition and annealing (SA_{BET}) and from broadening of XRD peaks we calculated average size of ZnO crystallites in each sample used for calorimetry.

ZnO–Silicycle interface area ($IA_{\text{SiO}_2\text{–ZnO}}$) per mol of ZnO can be calculated as (Fig. 4, Table I):

$$IA_{\text{SiO}_2\text{–ZnO}} = \frac{(x \cdot SA_{\text{SIL}}) + IA_{\text{ZnO(XRD)}} - SA_{\text{BET}}}{2}, \quad (1)$$

where $IA_{\text{ZnO(XRD)}}$ is the total interface area of ZnO, calculated assuming spherical crystallites with dimensions determined from XRD. ($x \cdot SA_{\text{SIL}}$) is surface area of Silicycle substrate per mol of deposited ZnO, and SA_{BET} is measured surface area of the sample after deposition, normalized per mol of ZnO.

Calculated $IA_{\text{ZnO–SIL}}$ for sample after 15 deposition cycles ZnO(15) is $\sim 8000 \text{ m}^2/\text{mol}$. For samples after 10 and 5 deposition cycles, ZnO(10) and Zn(5) calculations yield similar interface areas $\sim 11,000 \text{ m}^2/\text{mol ZnO}$. These data agree with similar crystallite size in ZnO(10) and ZnO(5) samples after annealing (Table I).

ZnO surface area (ZnO–air interface, SA_{ZnO}) in our samples can be calculated then as

$$SA_{\text{ZnO}} = IA_{\text{ZnO(XRD)}} - IA_{\text{SiO}_2\text{–ZnO}}. \quad (2)$$

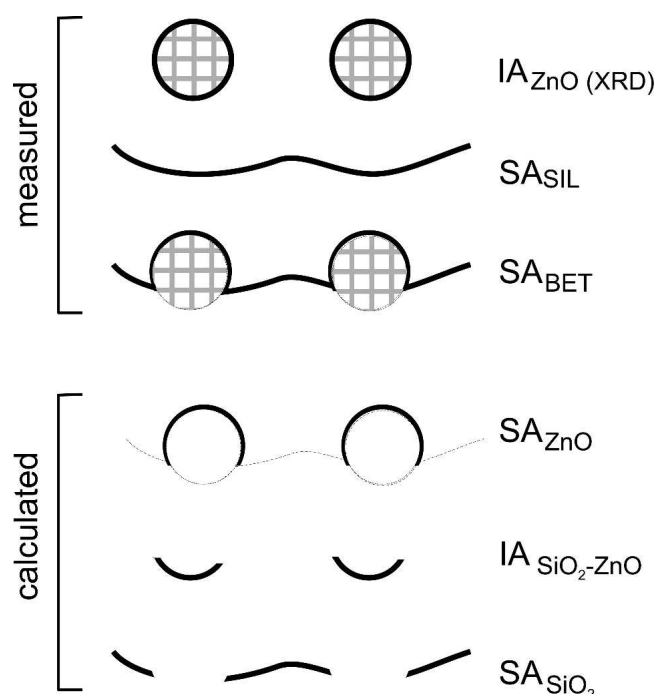


FIG. 4. Relations between measured and calculated interface areas for the case of ZnO particles formed on a Silicycle substrate. Filled circles represent ZnO particles. $IA_{\text{ZnO(XRD)}}$ is total interface area of ZnO particles determined from XRD, SA_{SIL} is surface area of uncovered Silicycle, and SA_{BET} is measured surface area of the sample after deposition. SA_{ZnO} , $IA_{\text{SiO}_2\text{–ZnO}}$, SA_{SiO_2} are calculated from Eqs. (1)–(3).

Surface area of Silicycle not covered with ZnO (SA_{SiO_2}) can be calculated as a difference between initial surface area of Silicycle substrate and interface area formed after annealing:

$$SA_{SiO_2} = x \cdot SA_{SIL} - IA_{SiO_2-ZnO} \quad (3)$$

The positive value SA_{SiO_2} of 12,500 m²/mol for ZnO(5) indicate that there is an insufficient quantity of ZnO crystals to cover all the substrate surface. For samples ZnO(15) and ZnO(10), the ZnO–Silicycle interface area calculated using Eq. (1) is larger than the total available substrate surface area, yielding in Eq. (3) negative SA_{SiO_2} values (Table III). This is indicative of formation of ZnO–ZnO interfaces. For these samples, SA_{ZnO} can be estimated from water adsorption experiments, since water adsorption on Silicycle surface is negligible compared with that on zinc oxide. In the sample after five deposition cycles, ZnO(5), the differential enthalpy of adsorption reaches the value of vapor condensation enthalpy (−44 kJ/mol) at 7.4 H₂O/nm² coverage. Assuming the same energetics of water adsorption as for ZnO(5), we calculated the surface areas of ZnO in ZnO(10) and ZnO(15) from the total amount of water adsorbed when the differential enthalpy of adsorption reaches −44 kJ/mol. The obtained area of ZnO (see Table III) is smaller than the total BET area of the sample indicating incomplete coverage of substrate.

Above calculations indicate that despite some ZnO–ZnO interfaces present in the samples after 10 and 15 deposition cycles, some uncovered Silicycle substrate was retained in these samples (Fig. 5). This could be explained by preferential coating of external pores of Silicycle during the ALD cycles.

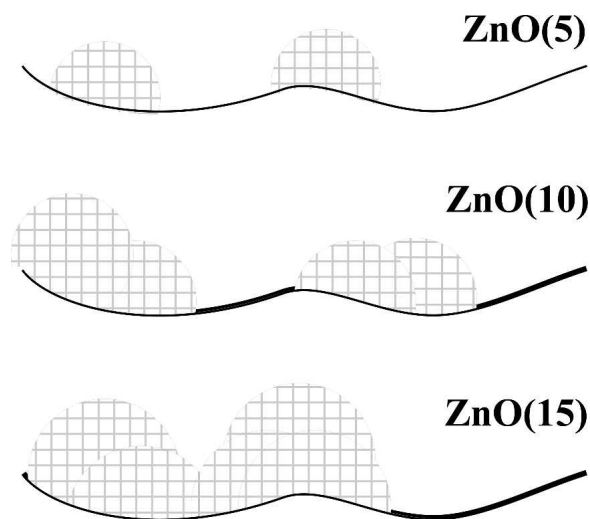


FIG. 5. Schematic representation of morphology of ZnO nanoparticles on the surface of amorphous silica substrate. Number of deposition cycles indicated in parentheses. Filled spheres represent crystallized ZnO nanoparticles.

D. Surface enthalpy

Surface enthalpy can be determined from calorimetric measurements by calculating excess enthalpy of the sample with respect to bulk material of the same structure, and dividing it by the surface area^{1–9}

$$\gamma = \frac{\Delta H_{\text{excess}}}{SA} \quad (4)$$

Excess enthalpies for hydrous and anhydrous surfaces for all crystalline samples are calculated using the thermochemical cycle and are given in Table IV. The details of these calculations are discussed elsewhere^{3–9,21} and are not repeated here.

In the sample with five deposition cycles ZnO(5), where formation of ZnO aggregates is unlikely, estimation of surface area of ZnO is most accurate. Thus, this sample will give most accurate estimation of surface enthalpy of ZnO prepared by ALD.

The data for our samples are compiled in Tables III, IV, and Fig. 6. The surface enthalpy for hydrous ZnO(5) is 1.23 ± 0.35 J/m². This value is in remarkable agreement with that reported earlier, 1.41 ± 0.05 J/m² for unsupported nanoparticles.⁹ For ZnO(5) with anhydrous surface our surface enthalpy is somewhat smaller than

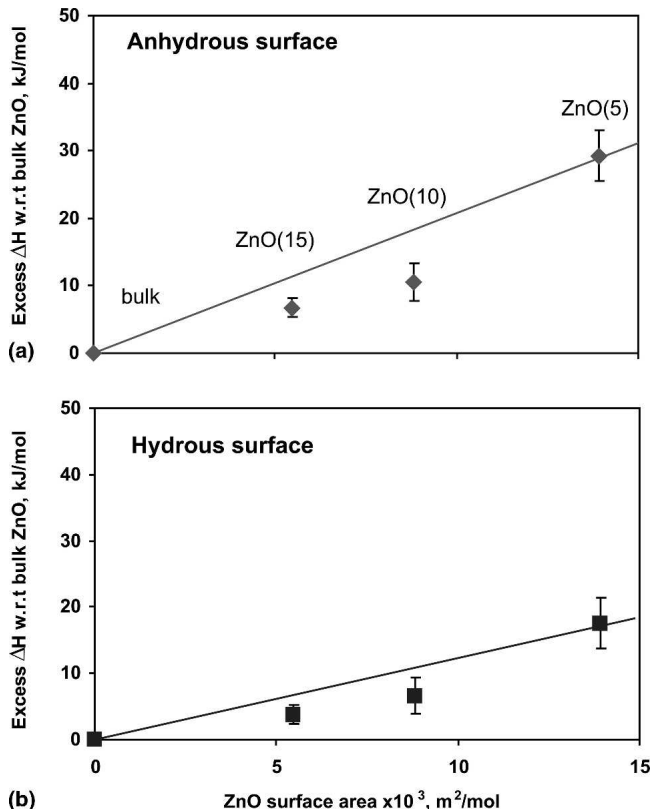


FIG. 6. Excess enthalpy of ZnO crystalline coatings relative to bulk ZnO as a function of surface area. (a) Anhydrous surface; (b) hydrous surface. Solid lines on the graphs corresponds to surface energies calculated based on ZnO(5) sample.

reported for ZnO nanoparticles⁹ ($2.07 \pm 0.59 \text{ J/m}^2$ versus $2.83 \pm 0.06 \text{ J/m}^2$). This could be caused by incomplete dehydration of the surface of ZnO in our samples, since some water is retained in Silicycle substrate at dehydration temperature. Another possible explanation is overestimate of preadsorbed water in ZnO nanoparticles due to ZnO sublimation in TG experiments.

It is remarkable that measured excess enthalpies for ZnO(15) and ZnO(10) are close to the above when only surface area of ZnO is taken into account. This indicates low interfacial energies for ZnO–ZnO interfaces present in these samples.

V. CONCLUSIONS

Calorimetric measurements of surface enthalpies of nanoparticles on a mesoporous substrate were performed for the first time. Enthalpies of crystalline interface for nonaggregated particles deposited on Silicycle by ALD are $1.23 \pm 0.35 \text{ J/m}^2$ and $2.07 \pm 0.59 \text{ J/m}^2$ for hydrated and anhydrous ZnO, respectively, and agree with data for unsupported ZnO. Water adsorption can be used for estimation of surface area of ZnO in the more complicated case of aggregate formation. There is higher water coverage on amorphous ZnO than on crystalline, perhaps indicating preferentially molecular water adsorption on its surface. Feasibility of thermochemical characterization of complex systems of ALD prepared particles on a substrate was demonstrated. Detailed study of energetics of amorphous zinc oxide that can be prepared by this technique is underway.

ACKNOWLEDGMENTS

This research was supported by Department of Energy (DOE) grant DE-FG0301ER15237. Some of this research was performed at Argonne National Laboratory, a United States Department of Energy Office of Science Laboratory operated under Contract No. DE-AC02-06CH11357 by UChicago, Argonne, LLC.

REFERENCES

1. L. Wang, K. Vu, A. Navrotsky, R. Stevens, B.F. Woodfield, and J. Boerio-Goates: Calorimetric study: Surface energetics and the magnetic transition in nanocrystalline CoO. *Chem. Mater.* **16**, 5394 (2004).
2. R.H.R. Castro, S.V. Ushakov, L. Gengembre, D. Gouvea, and A. Navrotsky: Surface energy and thermodynamic stability of γ -alumina. Effect of dopants and water. *Chem. Mater.* **18**, 1867 (2006).
3. M.W. Pitcher, S.V. Ushakov, A. Navrotsky, B.F. Woodfield, G. Li, J. Boerio-Goates, and B.M. Tissue: Energy crossovers in nanocrystalline zirconia. *J. Am. Ceram. Soc.* **88**, 160 (2005).
4. A.A. Levchenko, G. Li, J. Boerio-Goates, B.F. Woodfield, and A. Navrotsky: TiO₂ stability landscape: Polymorphism, surface energy, and bound water energetics. *Chem. Mater.* **18**, 6324 (2006).
5. L. Mazeina and A. Navrotsky: Surface enthalpy of goethite. *Clays Clay Miner.* **53**(2), 113 (2005).
6. L. Mazeina, S. Deore, and A. Navrotsky: Energetics of bulk and nano-akaganeite, β -FeOOH: Enthalpy of formation, surface enthalpy, and enthalpy of water adsorption. *Chem. Mater.* **18**, 1830 (2006).
7. J. Majzlan, L. Mazeina, and A. Navrotsky: Enthalpy of water adsorption and surface enthalpy of lepidocrocite (γ -FeOOH). *Geochim. Cosmochim. Acta* **71**, 615 (2007).
8. L. Mazeina and A. Navrotsky: Enthalpy of water adsorption and surface enthalpy of goethite (α -FeOOH) and hematite (α -Fe₂O₃). *Chem. Mater.* **19**, 825 (2007).
9. P. Zhang, F. Xu, A. Navrotsky, J.-S. Lee, S. Kim, and J. Liu: Surface enthalpies of nanophase ZnO with different morphologies. *Chem. Mater.* **19**, 5687 (2007).
10. S.V. Ushakov, A. Navrotsky, Y. Yang, S. Stemmer, K. Kukli, M. Ritala, M.A. Leskelä, P. Fejes, A. Demkov, C. Wang, B.-Y. Nguyen, D. Triyoso, and P. Tobin: Crystallization in hafnia- and zirconia-based systems. *Phys. Status Solidi B* **241**, 2268 (2004).
11. J.A. Libera, J.W. Elam, and M.J. Pellin: Conformal ZnO coatings on high surface area silica gel using atomic layer deposition. *Thin Solid Films* (in press).
12. J.M. Thomas and R. Raja: Catalytic significance of organometallic compounds immobilized on mesoporous silica: Economically and environmentally important examples. *J. Organometal. Chem.* **689**, 4110 (2004).
13. F.-S. Xiao: Ordered mesoporous materials with improved stability and catalytic activity. *Top. Catal.* **35**, 9 (2005).
14. J.H. Clark, D.J. MacQuarrie, and S.J. Tavener: The application of modified mesoporous silicas in liquid phase catalysis. *Dalton Trans.* **36**, 4297 (2006).
15. M. Kurtz, H. Wilmer, T. Genger, O. Hinrichsen, and M. Muhler: Deactivation of supported copper catalysts for methanol synthesis. *Catal. Lett.* **86**, 77 (2003).
16. S. Polarz, J. Strunk, V. Ischenko, M. Van den Berg, O. Hinrichsen, M. Muhler, and M. Driess: On the role of oxygen defects in the catalytic performance of zinc oxide. *Angew. Chem. Int. Ed. Engl.* **45**, 2965 (2006).
17. J. Tabatabaei, B.H. Sakakini, and K.C. Waugh: On the mechanism of methanol synthesis and the water-gas shift reaction on ZnO. *Catal. Lett.* **110**, 77 (2006).
18. S. Brunauer, D.L. Kantro, and C.H. Weise: The surface energies [enthalpies] of amorphous silica and hydrous amorphous silica. *Can. J. Chem.* **34**, 1483 (1956).
19. J.W. Elam, M.D. Groner, and S.M. George: Viscous flow reactor with quartz crystal microbalance for thin film growth by atomic layer deposition. *Rev. Sci. Instrum.* **73**, 2981 (2002).
20. J.M. Jensen, A.B. Oelkers, R. Toivola, D.C. Johnson, J.W. Elam, and S.M. George: X-ray reflectivity characterization of ZnO/Al₂O₃ multilayers prepared by atomic layer deposition. *Chem. Mater.* **14**, 2276 (2002).
21. J.W. Elam and S.M. George: Growth of ZnO/Al₂O₃ alloy films using atomic layer deposition techniques. *Chem. Mater.* **15**, 1020 (2003).
22. A. Navrotsky: Progress and new directions in high temperature calorimetry. *Phys. Chem. Miner.* **2**, 289 (1977).
23. A. Navrotsky: Progress and new directions in high temperature calorimetry revisited. *Phys. Chem. Miner.* **24**, 222 (1997).
24. S. Brunauer, P.H. Emmett, and E. Teller: Adsorption of gases in multimolecular layers. *J. Am. Chem. Soc.* **60**, 309 (1938).
25. E.P. Barret, L.G. Joyner, and P.B. Halenda: The determination of

- pore volume and area distributions in porous substances. I. Computations from nitrogen isotherms. *J. Am. Chem. Soc.* **73**, 373 (1951).
26. S.V. Ushakov and A. Navrotsky: Direct measurements of water adsorption enthalpy on hafnia and zirconia. *Appl. Phys. Lett.* **87**, 164103 (2005).
 27. J. Rouquerol, D. Avnir, C.W. Fairbridge, D.H. Everett, J.H. Haynes, N. Pernicone, J.D.F. Ramsay, K.S.W. Sing, and K.K. Unger: Recommendations for the characterization of porous solids. *Pure Appl. Chem.* **66**, 1739 (1994).
 28. M.A. Rodriguez, A. Navrotsky, and F. Licci: Thermochemistry of $\text{YBa}_2\text{Cu}_{3-x}\text{M}_x\text{O}_y$ ($\text{M} = \text{Ni}, \text{Zn}$). *Phys. C* **329**, 88 (2000).
 29. P.D. Maniar, A. Navrotsky, and C.W. Draper: Thermochemistry of the amorphous system silicon dioxide-germanium dioxide: Comparison of flame hydrolysis materials to high temperature fused glasses, in *Optical Fiber Materials and Processing*, edited by J.W. Fleming, G.H. Sigel, Jr., S. Takahashi, and P.W. France (Mater. Res. Soc. Symp. Proc., **172**, Pittsburgh, PA, 1990) p. 15.
 30. R.A. Robie and B.S. Hemingway: US Geol. Surv. Bull. Washington, DC, 2131 (1995).
 31. R.G. Gast, E.R. Landa, and G.W. Meyer: Interaction of water with goethite ($\alpha\text{-FeOOH}$) and amorphous hydrated ferric oxide surfaces. *Clays Clay Miner.* **22**, 31 (1974).